RE

Form Approved
OBM No. 0704-0188

1. Agency Use Only *(Leave blank).*

2. Report Date. 1992

Report Type and Dates Covered. Final - Proceedings

4. Title and Subtitle.
Physical optics and rigid/soft approximations to forward scattering by elastic shells

5. Funding Numbers.
Program Element No. 0602314N
Project No. 01451
Task No. JOC
Accession No. DN251108
Work Unit No. 94245E

6. Author(s).
Jacob George

7. Performing Organization Name(s) and Address(es).
Naval Research Laboratory
Ocean Acoustics Branch
Stennis Space Center, MS 39529-5004

8. Performing Organization Report Number.
PR 92:062:245

9. Sponsoring/Monitoring Agency Name(s) and Address(es).
Naval Research Laboratory
Center for Environmental Acoustics
Stennis Space Center, MS 39529-5004

10. Sponsoring/Monitoring Agency Report Number.
PR 92:062:245

11. Supplementary Notes.
Published in SPIE.

12a. Distribution/Availability Statement.
Approved for public release; distribution is unlimited.

12b. Distribution Code.

13. Abstract *(Maximum 200 words).*

Our numerical results demonstrate that both Fraunhofer and Fresnel diffractions provide good approximations to forward scattering by elastic spherical shells and rigid/soft spheres, for nondimensional frequency values $20<ka<80$, and scattering angles $0° < \theta < 10°$. There are only small differences among the Fraunhofer, Fresnel, and rigid/soft predictions for differential scattering cross sections. They arise mainly from the slightly varying degrees of compression (in angular space) of one pattern relative to another. The magnitudes of the maximums predicted by the four methods are in good agreement, but the minimums doe not agree. Calculations for 1%, 5%, and 10% spherical steel shells indicate that variation of shell thickness has only a small effect on forward scattering.

14. Subject Terms.
Signal processing, classification, antisubmarine warfare, underwater acoustics

15. Number of Pages. 13

16. Price Code.

17. Security Classification of Report.	18. Security Classification of This Page.	19. Security Classification of Abstract.	20. Limitation of Abstract.
Unclassified	Unclassified	Unclassified	SAR

Physical optics and rigid/soft approximations to forward scattering by elastic shells

Jacob George

Naval Research Laboratory, SSC Detachment, Code 245,
Stennis Space Center, MS 39529

ABSTRACT

Our numerical results demonstrate that both Fraunhofer and Fresnel diffractions provide good approximations to forward scattering by elastic spherical shells and rigid/soft spheres, for nondimensional frequency values $20 < ka < 80$, and scattering angles $0° < \theta < 10°$. There are only small differences among the Fraunhofer, Fresnel, and rigid/soft predictions for differential scattering cross sections. They arise mainly from the slightly varying degrees of compression (in angular space) of one pattern relative to another. The magnitudes of the maximums predicted by the four methods are in good agreement, but the minimums do not agree. Calculations for 1%, 5%, and 10% spherical steel shells indicate that variation of shell thickness has only a small effect on forward scattering.

1. INTRODUCTION

Forward scattering has been used in particle sizing in optical[1] and acoustic[2] measurements. Both Fraunhofer diffraction and Fresnel diffraction[3] have been used as predictive tools in calculations of scattering from objects of suitably small sizes. Since acoustic waves do penetrate elastic objects, but the Fraunhofer and Fresnel diffractions do not include elasticity, the validity of these physical optics approaches even in forward scattering may be questioned. In the present report we compare predictions of forward scattering from elastic spherical shells and rigid/soft spheres using known exact formulas,[4] to Fraunhofer and Fresnel predictions.

The methods of physical optics have been applied to acoustic scattering problems by many authors[2,5-12] with varying degrees of success. The most well known of these techniques is the Kirchhoff approximation (Ref. 5 and references therein). It assumes that the incident field and its normal derivative are unperturbed in an open aperture, and zero on the shadow side of a scatterer. Further, the outgoing signal on the insonified side of a scatterer is taken to be the incident signal multiplied by its plane wave reflection coefficient at every point on the scattering surface. The application of these assumptions to backscattering from semi-infinite plates,[5] and from spheres and cylinders[6-8] have shown that the Kirchhoff method is unreliable in these instances.

Applications of the Kirchhoff method to forward scattering problems have been more successful. Forward scattering from a semi-infinite plate has been discussed by Officer.[9] Pierce and Hadden find[10,11] that for small forward angles, the Kirchhoff method provides a good approximation to scattering by a wedge. This result is independent of the wedge angle. Hunter, Lee, and Waag[2] have experimentally measured forward scattering patterns of single nylon filaments. They demonstrated that the patterns were well explained by a Huygens construction, calculated numerically. The Fraunhofer and Fresnel calculations[3] discussed below are subsets (subsets that contain all the important elements) of the Huygens construction. In an earlier work,[12] this author compared the total field due to an infinite rigid cylinder at small forward angles calculated using exact formulas,[13] to that calculated using the Kirchhoff method adapted from Officer[9] for an opaque strip. The two predictions were in good agreement. For forward scattering, the Kirchhoff method is identical to Fresnel diffraction.[3,9] Since the concepts of Fresnel diffraction and Fraunhofer diffraction are well established as special cases of a unified theory based on the Fresnel-Kirchhoff integral,[3] we prefer to retain the Fresnel label instead of the Kirchhoff label. We show that in the examples considered here, both Fraunhofer diffraction and Fresnel diffraction provide good approximations to the scattered field as well as the total field due to elastic spherical shells and rigid/soft spheres.[14]

0-8194-0867-0/92/$4.00

2. EXACT FORMULAS

The well-known exact formulas[4] for spherical elastic and rigid/soft scatterers, are summarized in the present section. For spherical scatterers, the complex pressure of the incident plane wave can be written as

$$p_{inc} = \exp\,(ikr\cos\theta)\,, \tag{1}$$

where k is the wave number, r is the distance of the observation point from the center of the sphere, and θ is the spherical polar angle, with $\theta = 0$ for forward direction. Similarly for the scattered signal,

$$p_{scatt} = -\left(\frac{i}{kr}\right)\exp(ikr)\sum_{n=0}^{\infty}(2n+1)A_n P_n(\cos\theta) = \left(\frac{1}{r}\right)\exp(ikr)f(\Omega)\,. \tag{2}$$

Here, $P_n(\cos\theta)$ are the Legendre polynomials, and the coefficients A_n are determined from elastic boundary conditions.[4] The formulas are for the asymptotic case $kr >> 1$. For rigid/soft boundary conditions,[4]

$$A_n\ (\text{rigid}) = -\,j'_n(ka)/h'_n(ka),\ \text{and}\ A_n\ (\text{soft}) = -\,j_n(ka)/h_n(ka)\,. \tag{3}$$

Here the j_n are the spherical Bessel functions, and the h_n are the spherical Hankel functions of the first kind.

The differential scattering cross section in any direction Ω is given by

$$\left(\frac{d\sigma}{d\Omega}\right) = r^2\frac{|p_{scatt}|^2}{|p_{inc}|^2} = |f(\Omega)|^2\,. \tag{4}$$

The total field at any point is given by the coherent sum of incident and scattered fields as

$$p_{tot} = p_{inc} + p_{scatt}\,. \tag{5}$$

3. PHYSICAL OPTICS FORMULAS

In the physical optics approach to the forward scattering problem, we replace the scattering object (sphere) with an opaque screen having the same area of cross section. Consider the case when the wavefront due to the incident signal coincides with the screen (Fig. 1). We assume the signal and its derivative on the shadow side of the screen to be zero, as in the Kirchhoff method. The signal at every other point on the wavefront is assumed to be unperturbed. The complex pressure at any forward point is then given by the Fresnel-Kirchhoff integral[3]

$$p_{tot} = C' \iint_{\text{insonified}} \exp\,[ikf\,(\xi,\,\eta)]d\xi d\eta \tag{6}$$

where k is the wave number, the function $f(\xi,\eta) = [(r-r') + (s-s')]$ (Fig. 1), and the three-dimensional Cartesian coordinates of P', Q, and P are given by P'(x',y',z'), Q(ξ,η,0), and P(x,y,z). For incident plane waves of unit strength and small forward scattering angles, the constant C' is given by[3]

$$C' = -\,i\frac{k}{2\pi}\left[\frac{\exp(iks')}{s'}\right]. \tag{6a}$$

When the coordinates x', y', ξ, η, x, and y are small compared to both r' and s', we can expand $f(\xi,\eta)$ in a power series as

$$f(\xi,\,\eta) = -\,\frac{x'\xi + y'\eta}{r'} - \frac{x\xi + y\eta}{s'} + \frac{\xi^2 + \eta^2}{2}\left(\frac{1}{r'} + \frac{1}{s'}\right) + - - - -\,. \tag{7}$$

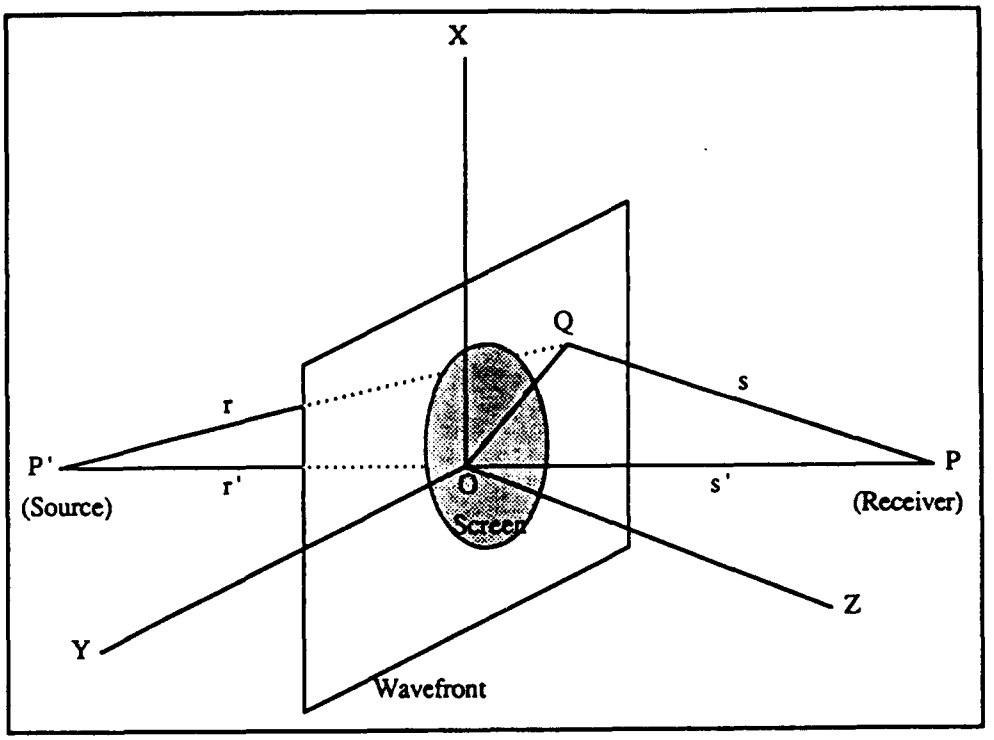

Fig. 1. Source, receiver, coordinate axes, and the position of the wavefront as it coincides with the screen.

The integral in Eq. (6) runs over the entire insonified region, viz. the wavefront extending to $+/-\infty$ in ξ and η, but excluding the opaque screen. (In the following we only evaluate integrals over a finite region of the wavefront, consistent with the condition of smallness of ξ and η relative to r' and s'.)

For better physical insight, let us rewrite Eq. (6) as

$$p_{tot} = C' \int_{-\infty}^{\infty}\int_{-\infty}^{\infty} \exp[ikf(\xi,\eta)]d\xi\,d\eta - C' \iint_{disc} \exp[ikf(\xi,\eta)]d\xi\,d\eta \equiv p_{inc} - p_{disc}, \tag{8}$$

where the integral labeled "disc" runs over the opaque screen. Equation (8) can be understood as a result of Babinet's principle.[3] The first term p_{inc} in Eq. (8) represents the field due to the entire infinite wavefront, the field in the absence of any scatterer. The second term p_{disc} in Eq. (8) represents the field due to the complementary geometry, an insonified opening in an infinite opaque screen.

The terms p_{tot} and p_{inc} in Eq. (8) have exactly the same meaning as the quantities p_{tot} and p_{inc} in Eq. (5) Therefore, the quantity $(-p_{disc})$ in Eq. (8) corresponds to the term p_{scatt} in Eq. (5). If both the diffraction theory and the scattering theory make identical predictions, then for the same incident field p_{inc} in Eqs. (5) and (8), $(-p_{disc})$ of Eq. (8) will be equal to p_{scatt} of Eq. (5) Following the scattering theory definition of differential scattering cross section in Eq. (4), we define the corresponding quantity for diffraction theory as

$$\left(\frac{d\sigma}{d\Omega}\right) = r^2 \frac{|p_{disc}|^2}{|p_{inc}|^2}. \tag{9}$$

When the quadratic and higher terms in $f(\xi,\eta)$ in Eqs. (6) and (7) can be ignored, we have the case of Fraunhofer diffraction.[3] Born and Wolf[3] demonstrate the condition for this as

$$r', s' >> \frac{(\xi^2 + \eta^2)_{max}}{\lambda} \tag{10}$$

where λ is the wavelength. When the quadratic terms are important, we have Fresnel diffraction.[3]

Let us now discuss the calculation of p_{inc} and p_{disc} of Eq. (8) under the two approximations. Evaluation of p_{disc} using Fraunhofer approximation poses no conceptual difficulty. Thus within the Fraunhofer approximation, using some change of variables and straightforward integration we obtain[3]

$$p_{disc}(\text{Fraunhofer}) = C' \iint_{disc} \exp\left[-ik\left(\frac{x'\xi + y'\eta}{r'} + \frac{x\xi + y\eta}{s'}\right)\right] d\xi d\eta$$

$$= -\frac{i}{2}\left[\frac{\exp(iks')}{ks'}\right](ka)^2\left[\frac{2J_1(ka \sin\theta)}{ka \sin\theta}\right]. \tag{11}$$

Here θ is the angular separation of a point on the diffraction pattern measured from the forward direction, and is the same as the angle θ in the previous section.

To calculate p_{disc} using the Fresnel approximation, Born and Wolf[3] choose a coordinate system such that the linear terms in $f(\xi,\eta)$ are identically zero. Then

$$f(\xi, \eta) = \frac{1}{2}\left(\frac{1}{r'} + \frac{1}{s'}\right)\left(\xi^2 \cos^2\delta + \eta^2\right) + - - - - , \tag{12}$$

where δ is the (small) angle between the line P'OP and the normal to the opaque screen. Defining new variables u and v, a new constant b', and indefinite integrals C_{uv}, and S_{uv} as

$$\frac{\pi}{2}u^2 = \frac{k}{2}\left(\frac{1}{r'} + \frac{1}{s'}\right)\xi^2 \cos^2\delta \tag{13a}$$

$$\frac{\pi}{2}v^2 = \frac{k}{2}\left(\frac{1}{r'} + \frac{1}{s'}\right)\eta^2 \tag{13b}$$

$$b' = \frac{\pi}{k(1/r' + 1/s')\cos\delta} \tag{13c}$$

$$C_{uv} \equiv \iint \cos\left[\frac{\pi}{2}(u^2 + v^2)\right] du\, dv \tag{13d}$$

$$S_{uv} \equiv \iint \sin\left[\frac{\pi}{2}(u^2 + v^2)\right] du\, dv, \tag{13e}$$

we can write

$$p_{disc}(\text{Fresnel}) = C' b' \iint_{disc} \exp\left[i\frac{\pi}{2}(u^2 + v^2)\right] du\, dv$$

$$= -\frac{i}{2}\exp(iks')\left[C_{uv}(disc) + iS_{uv}(disc)\right]. \tag{14}$$

Here, (disc) on the right hand side of Eq. (14) means that the integrals run over the opaque screen. Using trigonometric expansions of cosines and sines we obtain

$$C_{uv}(\text{disc}) = 2 \int_{\text{disc}} \cos\left(\frac{\pi}{2}u^2\right) C[v_{max}(u)]\,du - 2 \int_{\text{disc}} \sin\left(\frac{\pi}{2}u^2\right) S[v_{max}(u)]\,du \tag{15a}$$

$$S_{uv}(\text{disc}) = 2 \int_{\text{disc}} \sin\left(\frac{\pi}{2}u^2\right) C[v_{max}(u)]\,du + 2 \int_{\text{disc}} \cos\left(\frac{\pi}{2}u^2\right) S[v_{max}(u)]\,du \tag{15b}$$

where the line integral in the variable u runs from u_{min} to u_{max} (Fig. 2). The quantity v_{max} is given by

$$v_{max} = \left[a'^2 - (u + u_0)^2\right]^{1/2} \tag{16}$$

where

$$a' = \left[\frac{k}{\pi}\left(\frac{1}{r'} + \frac{1}{s'}\right)\right]^{1/2} a \tag{17}$$

is the reduced radius of the sphere in u-v space. The quantity u_0 is the (positive) distance in u-v plane between the origin of the coordinate system and the center of the opaque disc (Fig. 2). This distance is also equal to the distance

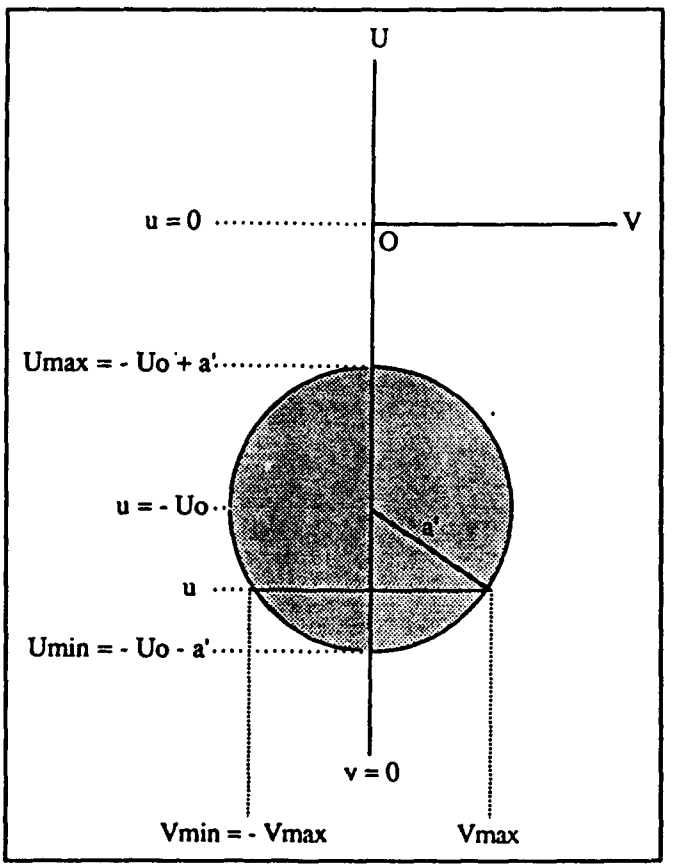

Fig. 2. The circular opaque screen (projection of sphere) in the u-v plane, as seen by an observer moving in the direction of the incident signal.

in the observation plane (also measured in reduced space) of a point on the diffraction pattern from the center of the pattern. Here we have approximated cos d by unity, using the fact that δ is very small. The quantities C and S are the well known Fresnel integrals[3] given by

$$C(x) = \int_0^x \cos\left(\frac{\pi}{2}u^2\right)du \tag{18a}$$

$$S(x) = \int_0^x \sin\left(\frac{\pi}{2}u^2\right)du\ . \tag{18b}$$

Formulas[15] to calculate C(x) and S(x) are given in Appendix A. We calculated C_{uv} (disc) and S_{uv} (disc) of Eqs. (14) and (15) by numerical integration using Simpson's rule.

The incident field p_{inc} is a plane wave of unit strength, given by

$$p_{inc}\ (\text{Fraunhofer}) = \exp\ (iks'\ \cos\ \theta) \tag{19}$$

in polar coordinates (s', θ), used in the Fraunhofer calculation. As mentioned above, the Fresnel calculation uses a special coordinate system[3] in which the diffracted field is calculated on a plane perpendicular to the incident signal direction, at distance s' from the scatterer. For this, the incident signal is given by

$$p_{inc}\ (\text{Fresnel}) = \exp\ (iks') \tag{20}$$

4. NUMERICAL RESULTS

Here we present the results of our calculation of differential scattering cross section and the total field based on the Fraunhofer and the Fresnel approximations. These results are compared with corresponding results obtained using exact formulas[4] for elastic spherical shells and rigid/soft spheres. In all examples, we have calculated the diffraction pattern in the far field, with $(s'/\lambda) = 1000$.

Figures 3–5 show the differential scattering cross section $d\sigma/d\Omega$ plotted vs. the forward scattering angle θ, for ka = 20, 40, and 80. There are only small differences among the Fraunhofer, Fresnel, and rigid/soft predictions for each case. They arise mainly from the slightly varying degrees of compression (in angular space) of one pattern relative to another. The magnitudes of the maximums predicted by the four methods are in good agreement, but the minimums do not agree.

Figures 6–8 show the squared magnitude of the total field p_{tot} plotted vs. the forward scattering angle θ, for ka = 20, 40, and 80. The total field p_{tot} was calculated for an incident field p_{inc} of unit strength. In each case, agreement among the Fraunhofer, Fresnel, and rigid/soft predictions is remarkably good. The diffraction pattern shows regularly spaced maximums and minimums. In all cases the asymptotic value (as θ increases) is 0 dB, consistent with the normalization of the incident signal strength to unity, and the fact that the scattered field strength falls off rapidly for increasing θ. The unit normalization of the incident signal also explains why the oscillations are centered at 0 dB.

The effect of shell thickness on forward scattering is illustrated in Fig. 9 for differential cross section $d\sigma/d\Omega$, and in Fig. 10 for the total field p_{tot}, for spherical steel shells of thicknesses 1%, 5%, and 10%. The ka value is 20 respectively. Fresnel and rigid/soft predictions are shown for comparison. Shell thickness has only a minimal effect in these examples.

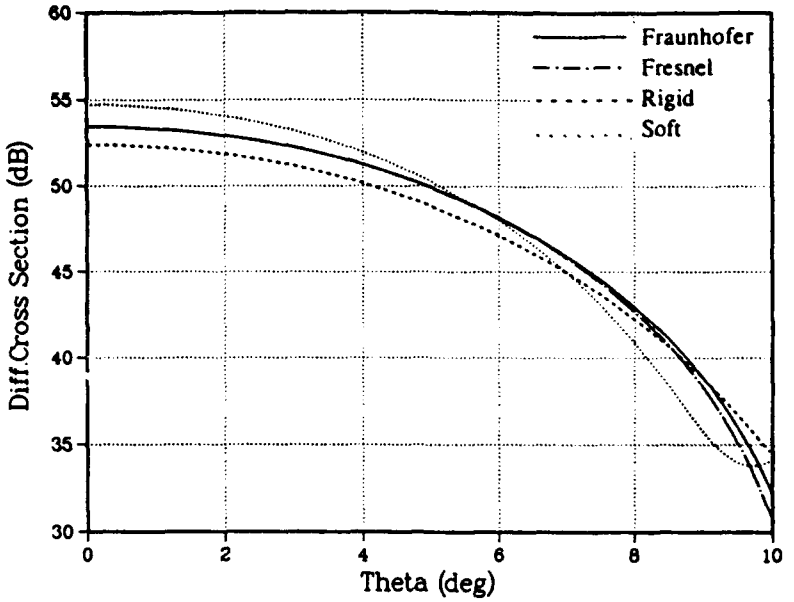

Fig. 3. Variation of differential scattering cross section $d\sigma/d\Omega$ with forward scattering angle θ for spherical rigid/soft spheres, compared with Fraunhofer and Fresnel diffractions. ka = 20.

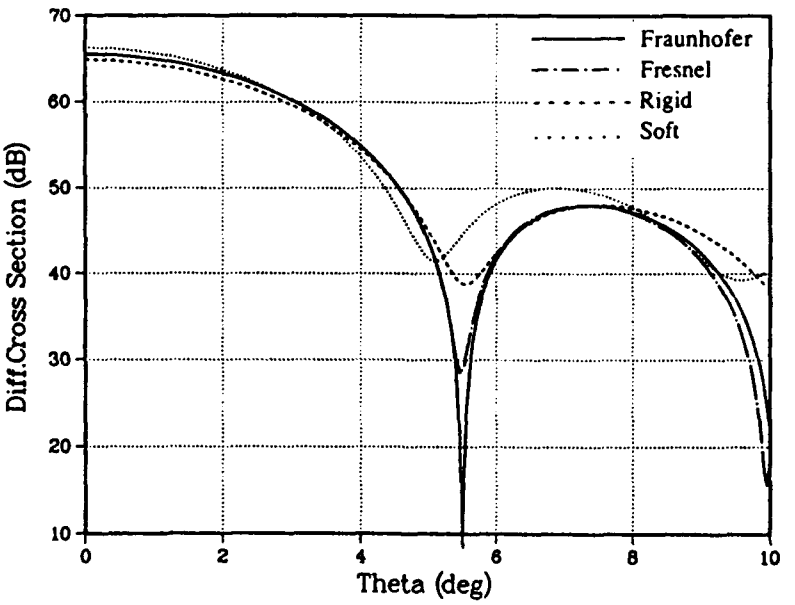

Fig. 4. Similar to Fig. 3, for ka = 40.

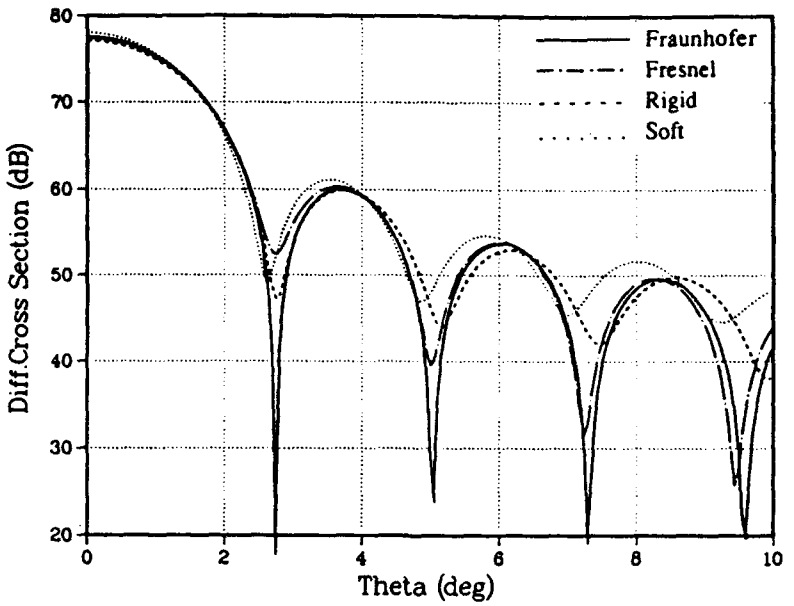

Fig. 5. Similar to Fig. 3, for ka = 80.

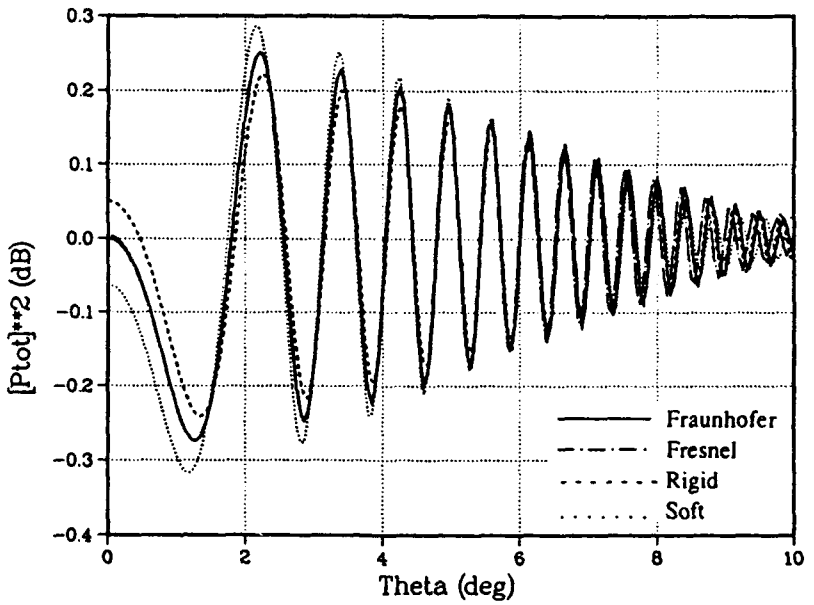

Fig. 6. Variation of the total acoustic field strength with forward scattering angle θ for spherical rigid/soft spheres, compared with Fraunhofer and Fresnel diffractions. ka = 20.

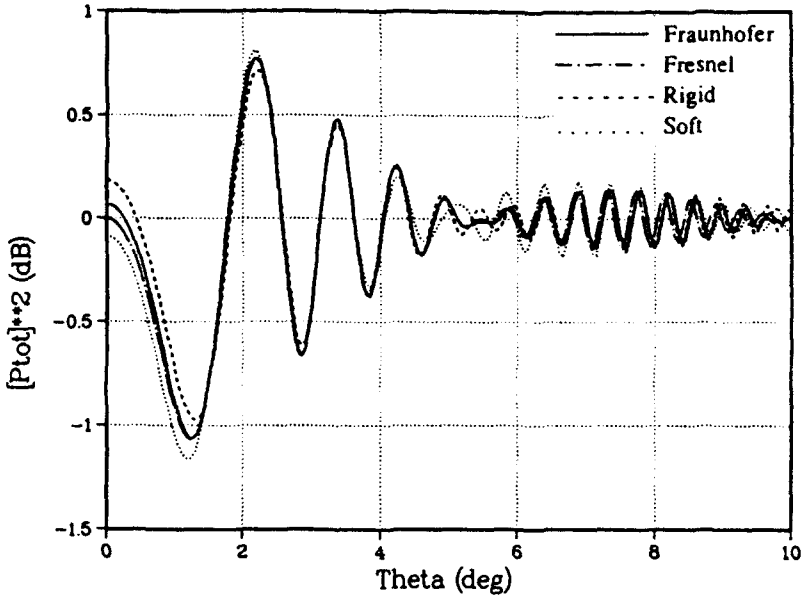

Fig. 7. Similar to Fig. 6, for ka = 40.

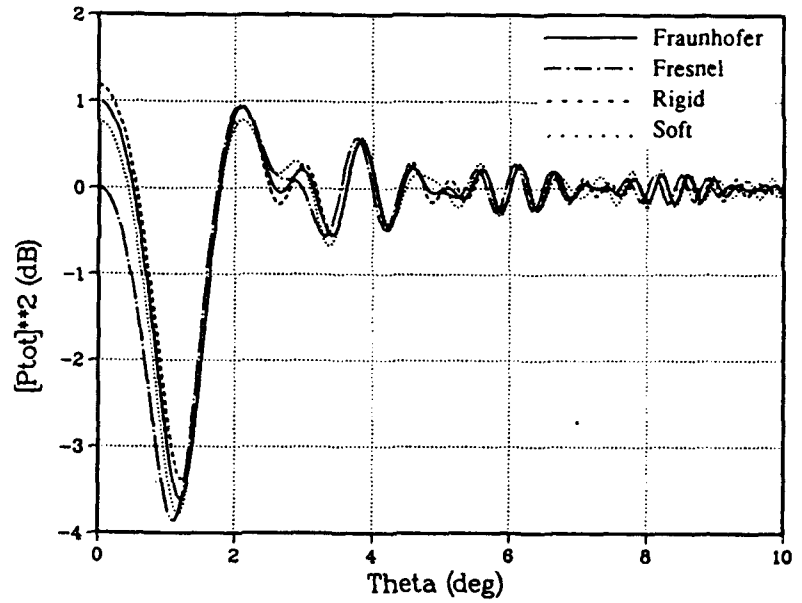

Fig. 8. Similar to Fig. 6, for ka = 80.

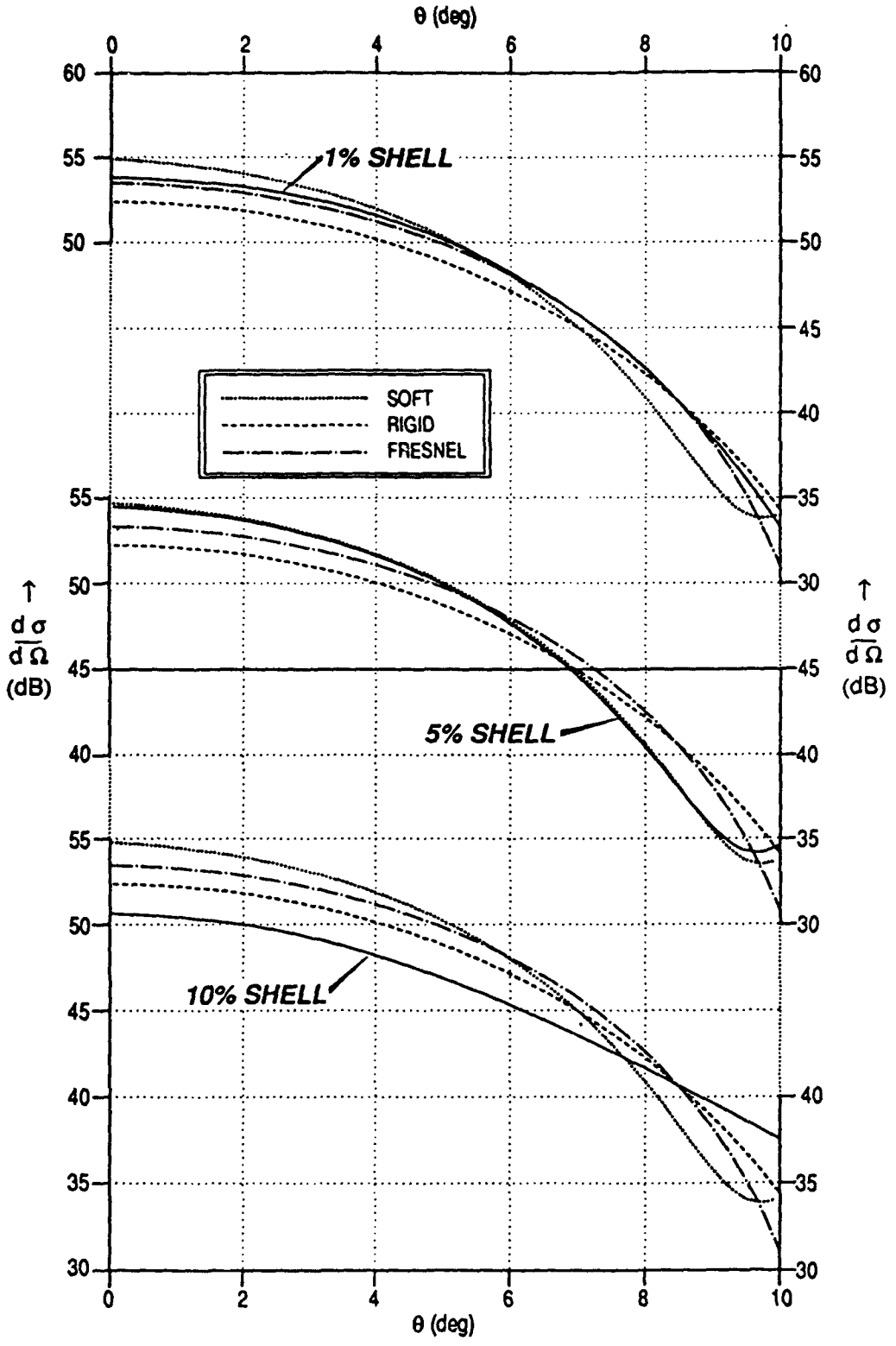

Fig. 9. Variation of differential scattering cross section $d\sigma/d\Omega$ with forward scattering angle θ for sphere. Results of 1% , 5%, and 10% steel shells are compared with rigid and soft body results, and Fresnel diffraction. ka = 20.

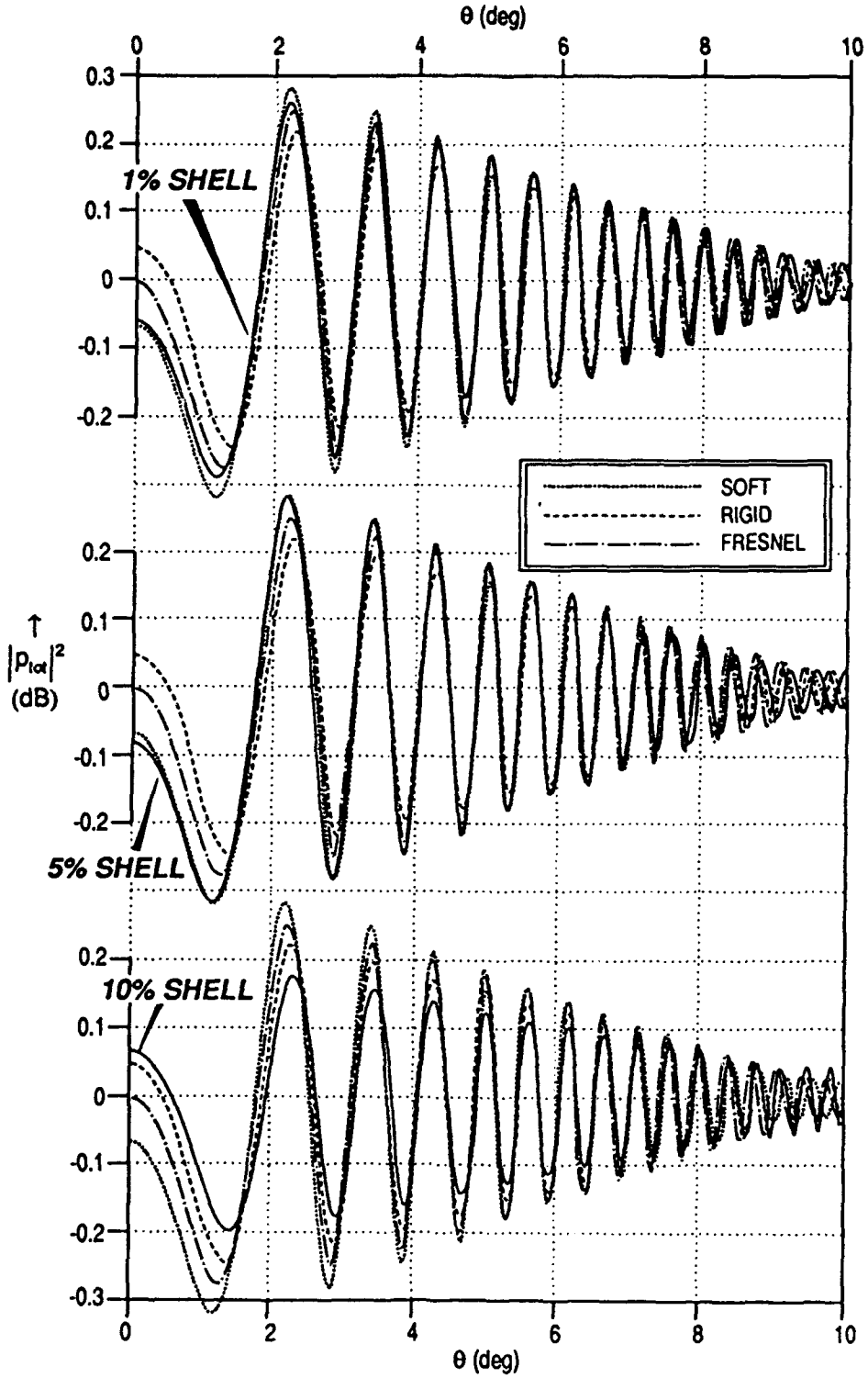

Fig. 10. Variation of the total acoustic field p_{tot} with forward scattering angle θ for sphere. Results of 1% , 5%, and 10% steel shells are compared with rigid and soft body results, and Fresnel diffraction. ka = 20.

5. CONCLUSIONS

Our numerical results demonstrate that both Fraunhofer and Fresnel diffractions provide good approximations to forward scattering by elastic spherical shells and rigid/soft spheres, for nondimensional frequency values $20 < ka < 80$, and scattering angles $0° < \theta < 10°$. There are only small differences among the Fraunhofer, Fresnel, and rigid/soft predictions for differential scattering cross sections. They arise mainly from the slightly varying degrees of compression (in angular space) of one pattern relative to another. The magnitudes of the maximums predicted by the four methods are in good agreement, but the minimums do not agree. Calculations for 1%, 5%, and 10% spherical steel shells indicate that variation of shell thickness has only a small effect on forward scattering.

6. ACKNOWLEDGMENTS

It is a pleasure to thank Prof. H. Überall for discussions, and Dr. Michael Werby for an elastic spherical shell computer program. Special thanks are due to the reviewer of a related JASA manuscript for pointing out the adequacy of the Fraunhofer approximation and for correcting an error in the derivation. Financial support for this work was provided by NRL program element 0601135N (Program Manager: Halcyon Morris). The computations were done on the VAX8650 computer at NRL. NOARL contribution number PR92:062:245.

APPENDIX A. FORMULAS TO CALCULATE FRESNEL INTEGRALS

For $x < 2.55$ we have used[15]

$$C(x) = \sum_{n=0}^{\infty} \frac{(-1)^n (\pi/2)^{2n} x^{4n+1}}{(2n)!(4n+1)}$$

$$S(x) = \sum_{n=0}^{\infty} \frac{(-1)^n (\pi/2)^{2n+1} x^{4n+3}}{(2n+1)!(4n+3)}.$$

For $x > 2.55$ we have used[15]

$$C(x) = \frac{1}{2} + f(x)\sin\left(\frac{\pi}{2}x^2\right) - g(x)\cos\left(\frac{\pi}{2}x^2\right)$$

$$S(x) = \frac{1}{2} - f(x)\cos\left(\frac{\pi}{2}x^2\right) - g(x)\sin\left(\frac{\pi}{2}x^2\right)$$

$$\pi x f(x) = 1 + \sum_{m=1}^{\infty} \frac{(-1)^m 1.3....(4m-1)}{(\pi x^2)^{2m}}$$

$$\pi x g(x) = \frac{1}{\pi x^2} + \sum_{m=1}^{\infty} \frac{(-1)^m 1.3....(4m+1)}{(\pi x^2)^{2m+1}}.$$

7. REFERENCES

1. J. Raymond Hodkinson, "Particle sizing by means of the forward scattering lobe," *Applied Optics*, 5, 839, 1966.

2. L. P. Hunter, P. P. K. Lee, and R. C. Waag, "Forward sound scattering by small nylon cylinders in water," *J. Acoust. Soc. Am.* 68, 314, 1980.

3. Max Born and Emil Wolf, *Principles of Optics*, pp. 375–386, and pp. 428–434, Pergamon, London, 1965.

4. R. R. Goodman and R. Stern, "Reflection and transmission of sound by elastic spherical shells," *J. Acoust. Soc. Am.* **34**, 338, 1962.

5. Gary M. Jebsen and Herman Medwin, "On the failure of the Kirchhoff assumption in backscatter," *J. Acoust. Soc. Am.* **72**, 1607, 1982.

6. Jacob George and H. Überall, "Approximate methods to describe the reflections from cylinders and spheres with complex impedance," *J. Acoust. Soc. Am.* **65**, 15, 1979.

7. C. S. Clay, "Low resolution acoustic scattering models: fluid-filled cylinders and fish with swim bladders," *J. Acoust. Soc. Am.* **89**, 2168, 1991.

8. Guillermo C. Gaunaurd, "Sonar cross sections of bodies partially insonified by finite sound beams," *IEEE J. Oceanic Eng.* **OE-10**, 213, 1985.

9. C. B. Officer, *Introduction to the Theory of Sound Transmission*, pp. 271–272, McGraw-Hill, New York, 1958.

10. Allan D. Pierce, "Diffraction of sound around corners and over wide barriers," *J. Acoust. Soc. Am.* **55**, 941, 1974.

11. W. James Hadden Jr. and Allan D. Pierce, "Sound diffraction around screens and wedges for arbitrary point source locations," *J. Acoust. Soc. Am.*, **69**, 1266, 1981.

12. ASA talk: Jacob George, "Diffraction of sound by an infinite rigid cylinder to small forward angles: a calculation using methods of physical optics," *J. Acoust. Soc. Am.* Vol. 70, Suppl. 1, p. 21, 1981.

13. R. D. Doolittle and H. Überall, "Sound scattering by elastic cylindrical shells," *J. Acoust. Soc. Am.* **39**, 272, 1966.

14. ASA talk: Jacob George and M. F. Werby, "Differential scattering cross sections at arbitrary outgoing angles and their relation to target boundary conditions," *J. Acoust. Soc. Am.* **89**, 1950, 1991.

15. Milton Abramowitz and Irene A. Stegun, *Handbook of Mathematical Functions*, pp. 301–302, Dover, New York, 1965.